X-ray Sensitivity Measurements of Charge Injection Devices (CID's)

Robert Forties
Laboratory for Laser Energetics
Summer High School Academic Program, August 2000

ABSTRACT

Charge injection devices (CID's) are digital cameras that can be used to directly image x-ray emission. The signal level from the CID can be related to the absolute x-ray flux provided an accurate calibration of the CID sensitivity as a function of photon energy is known. Measurements of the CID sensitivity at specific energies were made using energy dependent filters (Ross filters) and a laboratory x-ray source. These calibration values will be used in conjunction with values previously derived from comparison of CID and film images to obtain accurate measurements of image intensity and x-ray spectral intensity on the OMEGA laser.

INTRODUCTION

X rays are produced by illumination of targets by the OMEGA laser.[1] The laser beams compress and heat the targets creating short-lived ($\leq 1 \times 10^{-9}$ sec), high-temperature ($> 1 \times 10^{6}$ K) plasmas. Plasmas at these high temperatures emit x rays, which can be imaged. Regions of higher density and temperature emit more x rays, so an x-ray image of the target can reveal the symmetry of the implosion. Currently, film-based cameras are used to make images of target x-ray emission. The film has good resolution ($\leq 10\,\mu$m), and it has been calibrated so that the incident photon flux density can be measured. However, developing film is a lengthy process (taking about 40 minutes). Digitizing film to the accuracy needed for scientific work requires expensive equipment and adds much additional time to the process. Using film also requires loading and unloading from cameras in the target bay, developing, and digitizing. It is preferable to use digital cameras, which produce results almost instantaneously. CID cameras[2,3] are an example of a digital camera that has been used to make images of targets on OMEGA. Measurements of a CID camera's quantum efficiency have been made by comparison of CID and film recorded images, but further calibration is needed.[4]

The subject of this paper is the measurement of the response of the CID cameras to x-rays at several different energies. Since the camera sensitivity varies as a function of x-ray energy, energy dependent measurements are needed. To calibrate a camera, a nearly monochromatic beam of x rays is needed. Monochromatic radiation contains

photons that are all of the same energy. X rays can be produced by high-energy electrons striking a solid target. When subjected to electrons at a high enough voltage, the target will emit an x-ray spectrum that contains several emission lines. An associated continuous spectrum of radiation is produced by electrons that are deflected by the atoms of the target and give off part of their energy in the form of an x ray.[5, 6] Using pairs of filters (Ross filters)[7,8] a narrow, nearly monochromatic x-ray flux was produced and used to calibrate a CID camera.

EXPERIMENTS

Measurements were conducted in air using an X-TECH model 1303 sealed Cu-tube x-ray source.[9] X rays from the X-TECH source passed through a lead-lined collimator and filter box impinging on either a CID camera or a lithium drifted silicon detector (abbreviated Si(Li) detector), which is an accurate photon counter.[10] Both detectors were mounted on a computer-controlled table to allow precise positioning. The total distance from the source aperture to the recording device was 16 cm. A diagram of the setup used for experiments is shown in Figure 1.

Filters were used to measure the response of the camera in a narrow energy band. The x-ray emission was filtered using two filters, one having a K-shell absorption edge just below the desired energy and the other having a K-shell absorption edge just above the desired energy. The thicknesses of the filters were calibrated so that the transmission of the filters was nearly equal except in the region between their K absorption edges. In this region, called the pass band, the first filter strongly absorbed the x-rays (including the $K\alpha$ emission) and the second strongly transmitted them. This technique is known as Ross

filtering.[7, 8] Figure 2 shows the transmission for a sample set of filters. The response of the camera to x rays transmitted through both filters was measured, and then subtracted. The difference between the responses of the camera to the two filters is due almost entirely to the energies within the pass band. There is some error in this method because the transmission of the filters cannot be perfectly matched for the regions outside the pass band, so some of the difference in the responses is due to radiation outside the desired region. Also, the pass band includes radiation in a narrow region, not a single energy, and therefore is not strictly monochromatic. However, the result is much more monochromatic than that which can be achieved with a single filter.

To compute the quantum efficiency of the CID from the measurements the flux reaching the camera and the Si(Li) detector was assumed to be the same. Since the CID measures energy, the flux it measures in units of photons/($\mu m^2 \times$ sec) can be expressed as

$$\phi_{CID} = \frac{\Delta N_{ADU} / E_{photon}}{A_{pixel}\ \Delta t_{exposure}\ T_{Win}(E)\ QE_{CID}} \times C\ , \qquad (1)$$

where ΔN_{ADU} is the number of "analog-to-digital-units" (ADU's) recorded by the CID, T_{Win} is the transmission of the Be window covering the camera at energy E, which is assumed to be nearly one, $\Delta t_{exposure}$ is the exposure time for the CID in seconds, A_{pixel} is the area of a CID pixel (1482 μm^2, assuming a 38.5 μm square pixel), QE_{CID} is the quantum efficiency of the CID, E_{photon} is the mean energy of the incident photons in keV/photon, and C is a constant that converts ADU's to keV.

Since the Si(Li) detector is a photon counter, the flux it measures in photons/(μm^2 × sec) can be expressed by

$$\phi_{Si(Li)} = \frac{\Delta N_{counts}}{A_{pin}\ \Delta t_{int}\ \varepsilon_{Si(Li)}(E)}\ , \qquad (2)$$

Where ΔN_{counts} is the number of photons recorded by the Si(Li) detector, $\varepsilon_{Si(Li)}(E)$ is the efficiency of the Si(Li) detector at energy E including the transmission of the Be window covering it (which are collectively assumed to be nearly 1), A_{pin} is the area of the pinhole in front of the Si(Li) detector in μm, and Δt_{int} is the exposure time for the Si(Li) detector in seconds. The equations for the flux on both detectors may then be set equal to each other and solved to find the quantum efficiency of the CID, resulting in

$$QE_{CID} = \frac{\dfrac{\Delta N_{ADU}/E_{photon}}{A_{pixel}\ \Delta t_{exposure}\ T_{Win}(E)}}{\dfrac{\Delta N_{counts}}{A_{pin}\ \Delta t_{int}\ \varepsilon_{Si(Li)}(E)}} \times C. \qquad (3)$$

RESULTS

Lower energy measurements were taken using a 25-μm thick Sc filter and 100-μm thick Polyvinylidene chloride (PVDC) filter to create a difference spectrum with an average energy of 4.06 keV. Both measurements were made with the X-TECH source set

to 9 kV and 0.19 mA, and with a lead pinhole in front of the Si(Li) detector. Figure 3(a) shows the results of the Si(Li) from these measurements, and Figure 3(b) shows the difference spectrum resulting from Sc and PVDC filters. Average lineouts of the CID response at 4.06 keV are shown in Figure 4. For higher energy measurements a 10-μm thick Ni filter and a 15-μm thick Fe filter were used to isolate the copper Kα emission, which has an energy of 8.04 keV. One measurement was taken with the X-TECH source set to 19 kV and 0.10 mA and a pinhole in a 10-μm thick Pt substrate over the Si(Li) detector and a 50.8 μm Al filter to reduce low-energy noise. The results of these measurements are shown in Figure 5 for the Si(Li) detector and Figure 6 for the CID. The other 8.04 keV measurement was taken at 19 kV and 0.19 mA with a pinhole in a Pb substrate over the Si(Li) detector and a 101.6 μm aluminum filter. A background was taken for each CID image and then subtracted from the corresponding image. After the remaining background was set to zero, the image was then corrected to compensate for continued exposure of the camera to radiation during the readout phase using the readout rate of 0.5 MHz and assuming that it is only sensitive during half of each phase of the readout cycle. The image produced by the difference between CID measurements with Fe and Ni filters is shown in Figure 7. A CID 4150[2] was used for all experiments, and was read out with a 12-bit GAGE digitizer card.[11] The Si(Li) detector measurement was made using an AMPTEK XR-100CR x-ray detector and a PX2T/CR amplifier[12] with the gain set to 3.0.

Table 1 shows all data obtained from experiments. The results are listed by filter pair used to obtain the desired x-ray energy, with the filter absorbing at that energy listed

first (Filter A) and the filter transmitting the desired energy listed second (Filter B). QE_{CID} is the quantum efficiency of the CID calculated using equation 3.

If the proportionality constant (C) in equation 3 is set to 1.31, the data from this experiment can be normalized to the known absorption of a 7-μm thick Si depletion region covered by an electrically inactive layer with an absorption equivalent to 1 μm of Si.[13] The known absorption curve is compared to normalized data in Figure 8(a). In addition, Figure 8(b) shows that, when calibrated with this same constant, the data follows a curve of CID quantum efficiency generated by comparison of CID and film images of grating-dispersed x-rays[4] (although some uncertainty in the absolute quantum efficiency still remains due to uncertainty in the value of C).

CONCLUSIONS

Measurements of CID quantum efficiency as a function of energy have been made with Ross filters by comparing the response of a CID to x rays with that of a Si(Li) detector. These measurements follow the trend expected based on the known absorption of silicon and assumed dead layer and depletion layer thicknesses. These measurements also agree in trend with a previous CID calibration made by comparison of CID and film images. However the proportionality constant needed to calculate CID quantum efficiency is not well known, so it is only possible to verify that the ratios between the measurements at different energies are correct. Estimates of the absolute quantum

efficiency therefore have some remaining uncertainty which could be minimized by further measurements.

ACKNOWLEDGEMENTS

I would most of all like to thank my advisor Dr. Frederick J. Marshall for all of his help and support throughout this project. I would also like to thank Dr. R. Steven Craxton and the Laboratory for Laser Energetics for their support of the summer high school academic program and Tom Ohki for his help at the beginning of the summer.

REFERNCES

1. T. R. Boehly, D. L. Brown, R. S. Craxton, R. L. Keck, J. P. Knauer, J. H. Kelly, T. J. Kessler, S. A. Kumpan, S. J. Loucks, S. A. Letzring, F. J. Marshall, R. L. McCrory, S. F. B. Morse, W. Seka, J. M. Soures, and C. P. Verdon. *Opt. Commun.* **133**, 495 (1997).
2. CID technologies, Inc., 101 Commerce Blvd., Liverpool, NY 13088.
3. J. Carbone, Z. Alam, C. Borman, S. Czebiniak and H. Ziegler. *Proceedings of SPIE,* **3301**, 90 (1998).
4. F. J. Marshall and T. Ohki, accepted for publication *Rev. Sci. Instrum.,* to appear in **Special Issue, 13th Conference on High Temperature Plasma Diagnostics, Tucson, AZ** (June 2000).
5. B. D. Cullity. Pages 7-12 and 21-27 of *Elements of X-ray Diffraction,* (Reading, Massachusetts: Addison-Wesley, 1978).
6. Harold P. Klug and Leroy E. Alexander. Pages 60-79 of *X-ray Diffraction Procedures* (New York: Wiley, 1974).
7. B. D. Cullity. Pages 19-21 and 227-229 of *Elements of X-ray Diffraction,* (Reading, Massachusetts: Addison-Wesley, 1978).
8. Harold P. Klug and Leroy E. Alexander. Pages 105-107 of *X-ray Diffraction Procedures* (New York: Wiley, 1974).
9. X-TECH Co., W. Hershyn Co.'s Inc., 1570 Soquel Dr., Santa Cruz, CA 95065.
10. B. D. Cullity. Pages 210-213 of *Elements of X-ray Diffraction,* (Reading, Massachusetts: Addison-Wesley, 1978)

11. Gage Applied Sciences, Inc., 2000, 32nd Ave., Lachine Montreal, QC Canada, H8T 3H7.

12. AMPTEK, Inc., 6 De Angelo Drive, Bedford, Mass. 01730.

13. B. L. Henke, E. M. Gullikson, and J. C. Davis, *At. Nucl. Data Tables*, **54**, 181 (1993)

FIGURE CAPTIONS

Figure 1. Diagram of the setup used for taking measurements. The collimator and filter holder were both lead lined to prevent x-ray leakage. All elements were mounted on an optical table.

Figure 2. Plot of the transmission of Fe and Ni filters. The filter transmission is almost identical except in the pass band. Thus, when the camera responses to the two filters are subtracted, the difference is due almost entirely to x rays with energies falling in the pass band. This filter pair was used to isolate the Cu Kα line.

Figure 3. Si(Li) detector data from Sc and PVDC filtered x-ray spectra. (a) Sc and PVDC filtered spectra plotted with the unfiltered spectrum; (b) difference spectrum for Sc and PVDC filters.

Figure 4. CID response to PVDC and Sc filtered x-ray spectra averaged across columns 200 to 300, plotted with the difference spectrum.

Figure 5. Si(Li) detector data from Fe and Ni filtered x-ray spectra. (a) Fe and Ni filtered spectra plotted with the unfiltered spectrum; (b) difference spectrum from Fe and Ni filters.

Figure 6. CID response to Fe and Ni filtered x-ray spectra averaged across columns 200 to 300, plotted with the difference between the two responses.

Figure 7. Image produced by the difference between CID images of Fe and Ni filtered x-ray spectra.

Figure 8. Quantum efficiencies calculated from results: (a) shown normalized at 4.06 keV to the known absorption of 7-μm of Si with a 1-μm Si dead layer; (b) plotted with an efficiency curve obtained by comparison of CID and film images.[4]

Table 1

Filters (A/B)	Mean Energy (keV)	Si(Li) Δt_{int} (sec)	Si(Li) Detector			Si(Li) Flux $\left(\frac{\text{Photons}}{\mu m^2 \times sec}\right)$	ΔA_{pin} Si(Li) (μm^2)	CID Δt_{exp} (sec)	CID Camera			QE_{CID}
			N Filter A (Counts)	N Filter B (Counts)	ΔN (B-A) (Counts)				N Filter A (ADU's)	N Filter B (ADU's)	ΔN (B-A) (ADU's)	
PVDC/ Sc	4.06	200	12	3570	3558	0.0100	1770	2	30	75	45	0.49
PVDC/ Sc	4.06	200	14	3789	3775	0.0107	1770	2	23	64	41	0.42
Fe/Ni + 50.8 μm Al	8.04	100	498	2212	1714	0.2417	70.9	1	106	282	176	0.080
Fe/Ni + 101.6 μm Al	8.04	200	11008	57883	46875	0.1324	1770	2	64	263	199	0.083

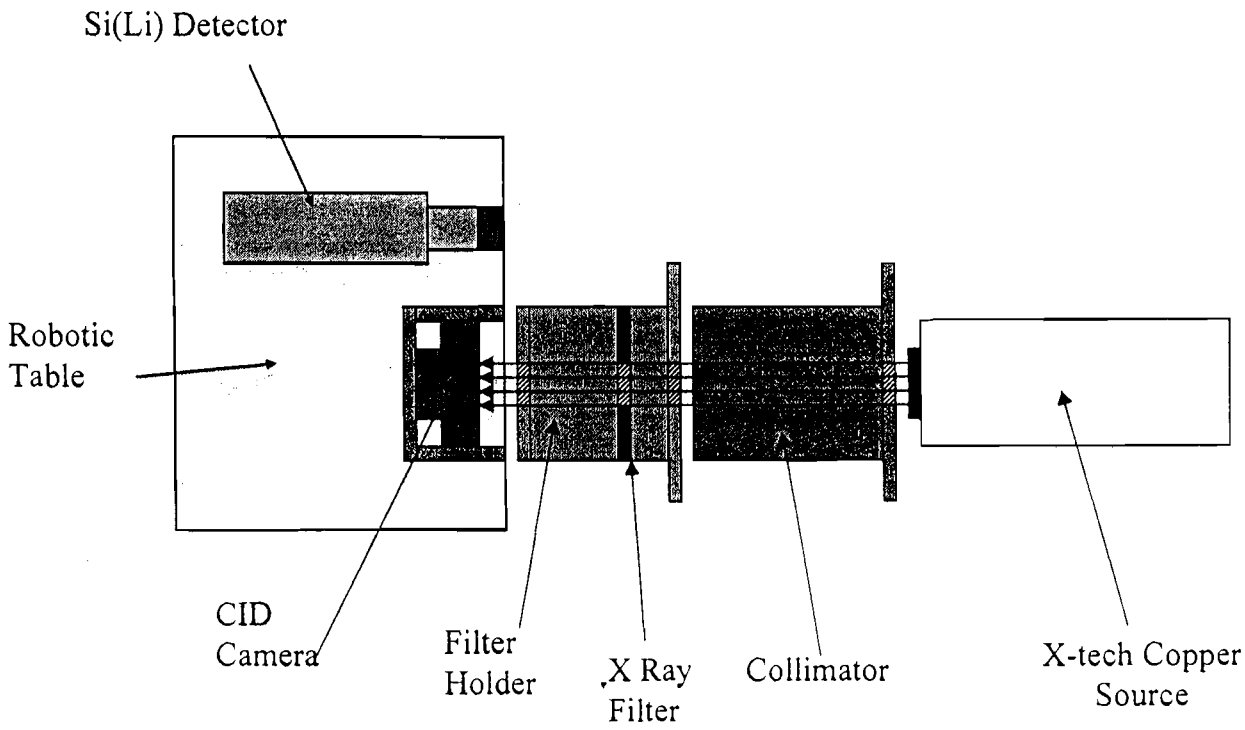
Si(Li) Detector
Robotic
Table
CID
Camera
Filter
Holder
X Ray
Filter
Collimator
X-tech Copper
Source

Figure 1

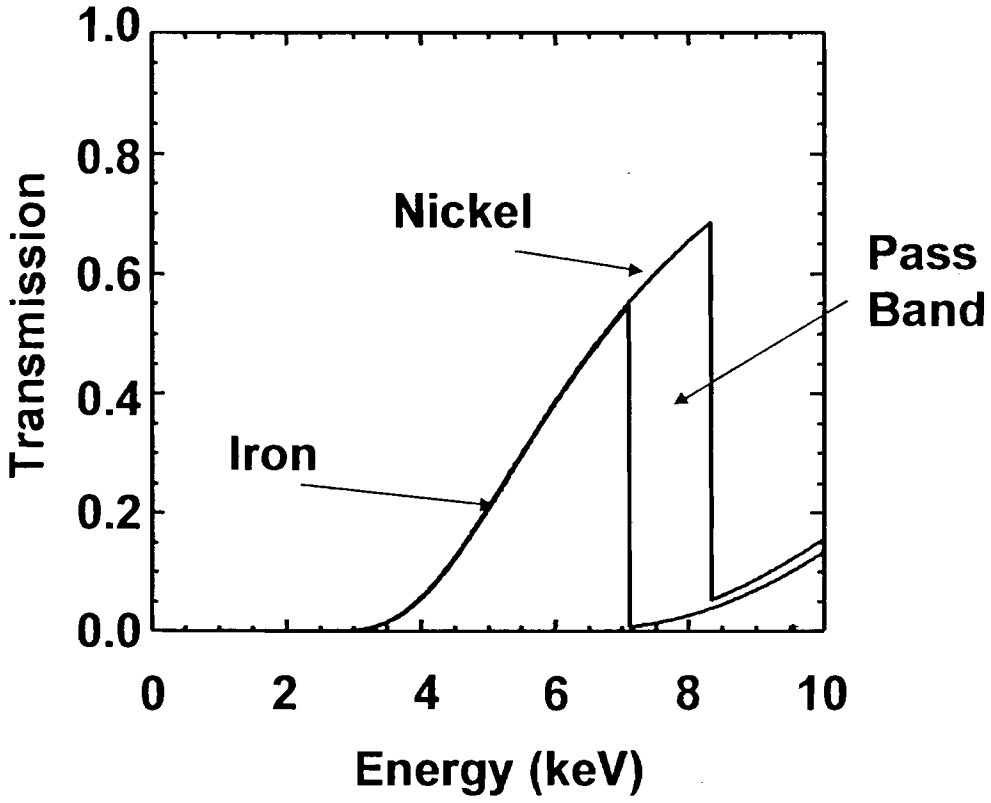
1.0
0.8
0.6
0.4
0.2
0.0
Transmission
Nickel
Pass
Band
Iron
0
2
4
6
8
10
Energy (keV)

Figure 2

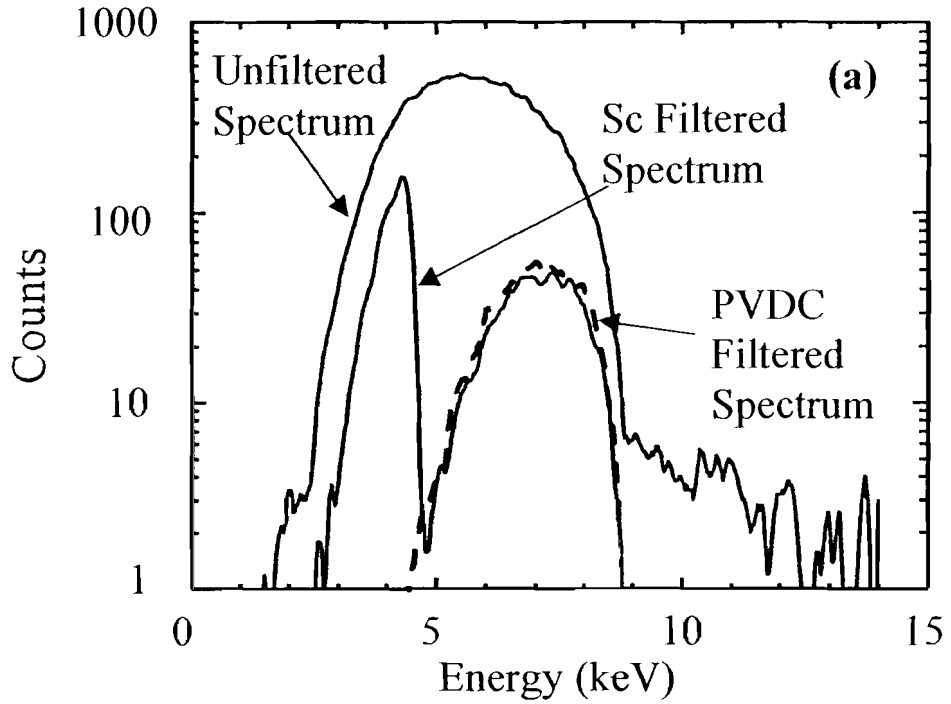
1000
100
10
1
Counts
Unfiltered
Spectrum
Sc Filtered
Spectrum
PVDC
Filtered
Spectrum
(a)
0
5
10
15
Energy (keV)

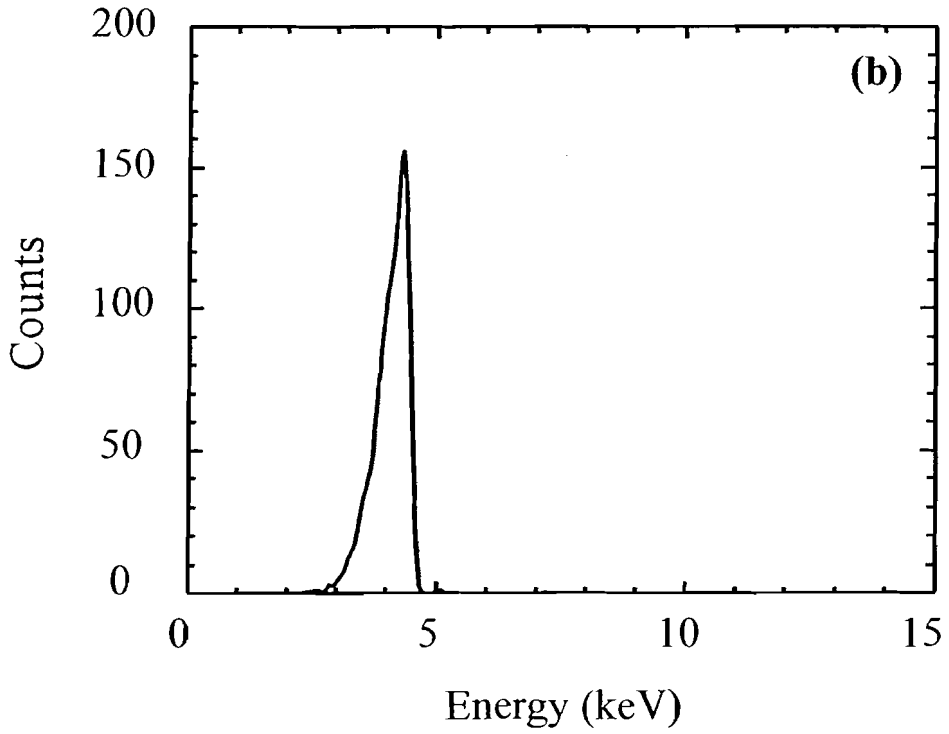
200
150
100
50
0
Counts
(b)
0
5
10
15
Energy (keV)

Figure 3

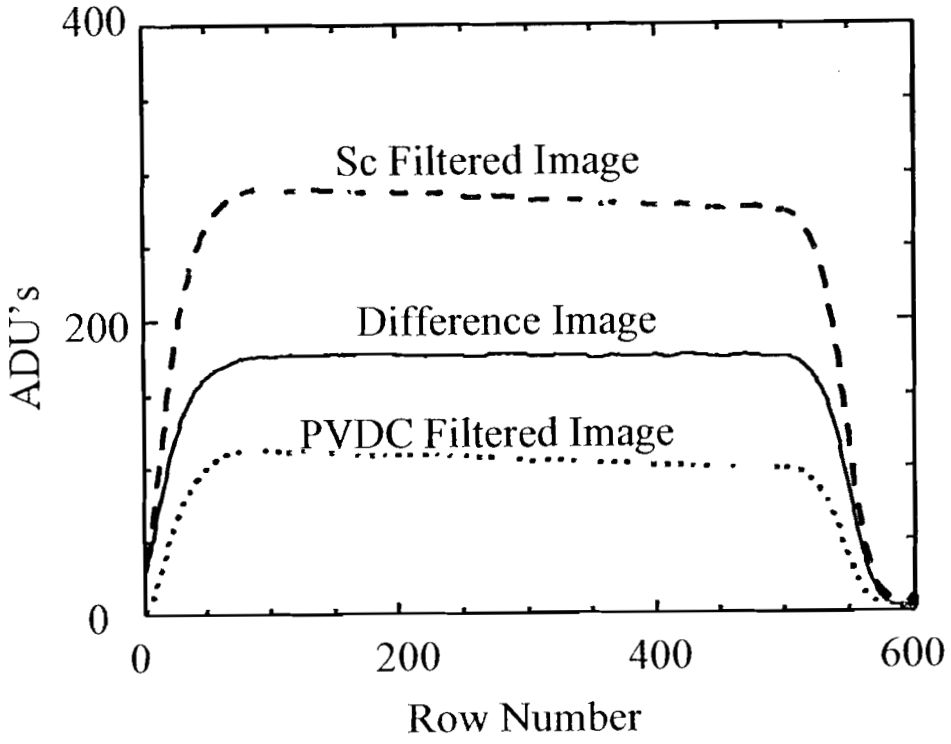
400
200
0
ADU's
Sc Filtered Image
Difference Image
PVDC Filtered Image
0
200
400
600
Row Number

Figure 4

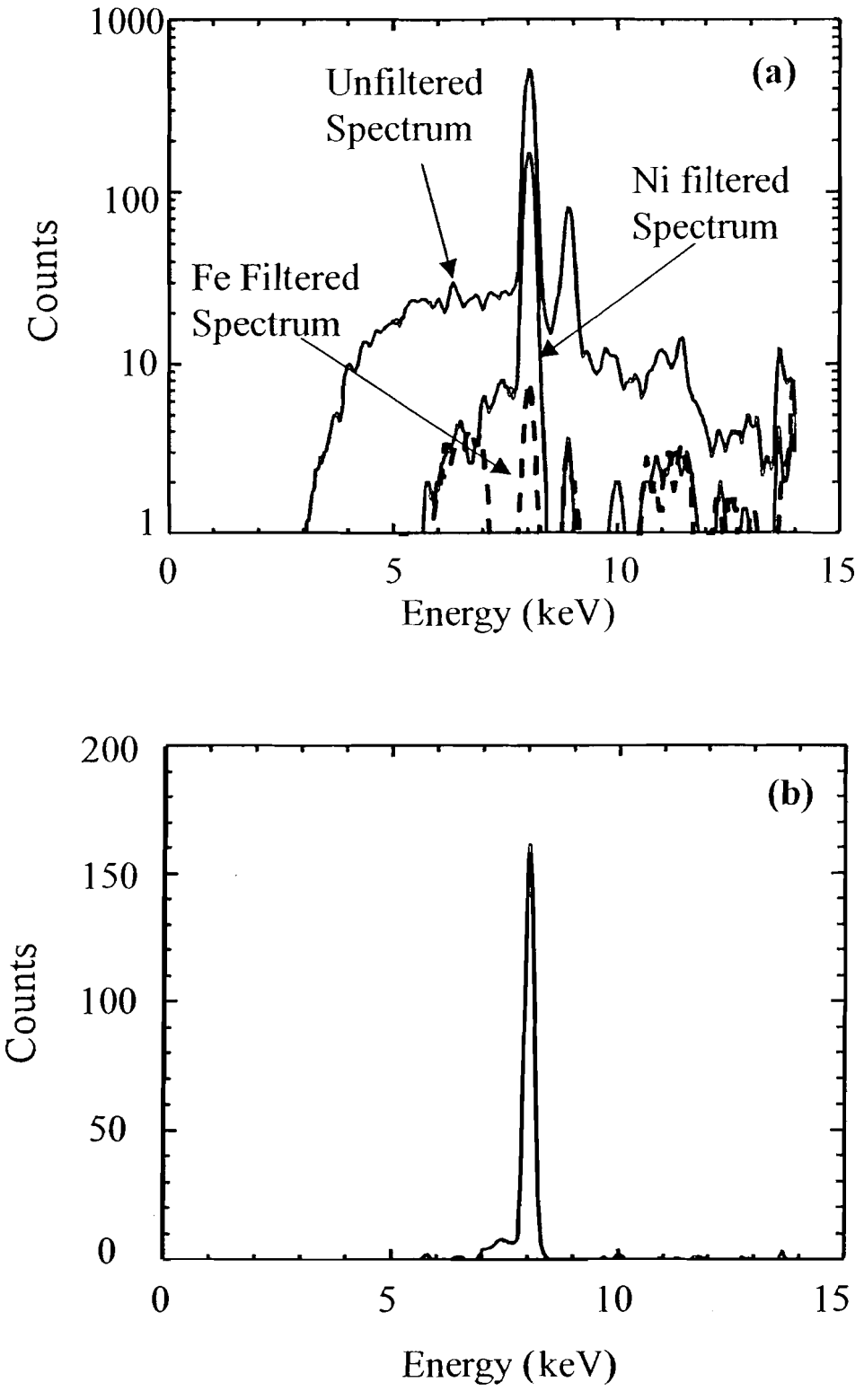
1000
100
10
1
Counts
(a)
Unfiltered
Spectrum
Ni filtered
Spectrum
Fe Filtered
Spectrum
0
5
10
15
Energy (keV)
200
150
100
50
0
Counts
(b)
0
5
10
15
Energy (keV)

Figure 5

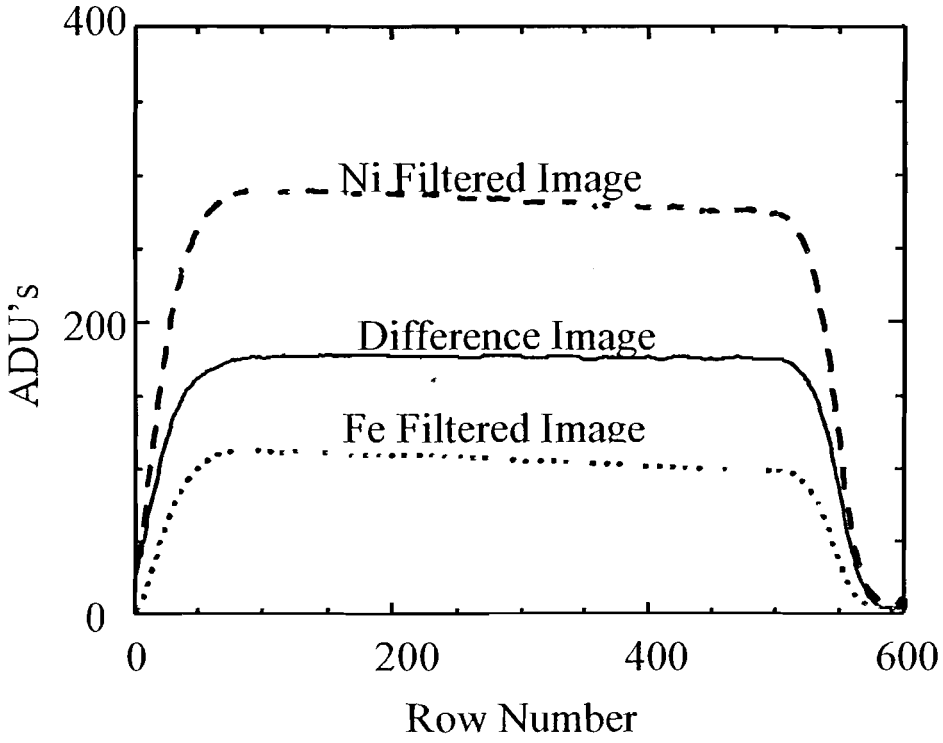
400
200
0
ADU's
Ni Filtered Image
Difference Image
Fe Filtered Image
0
200
400
600
Row Number

Figure 6

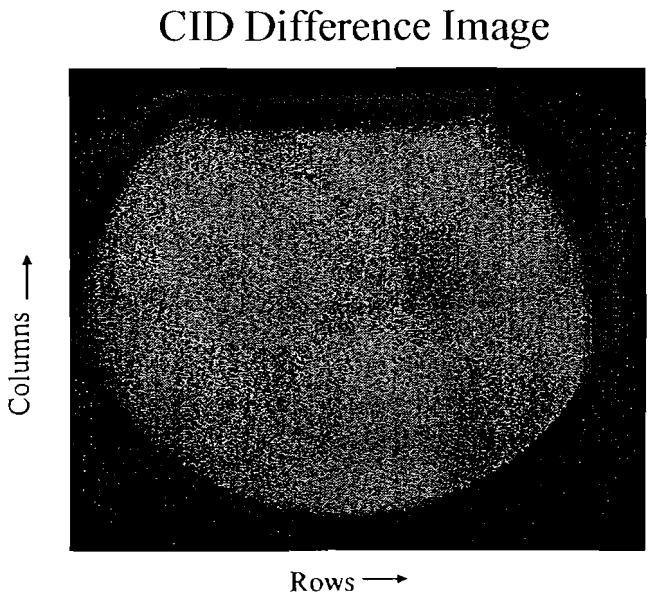

Figure 7

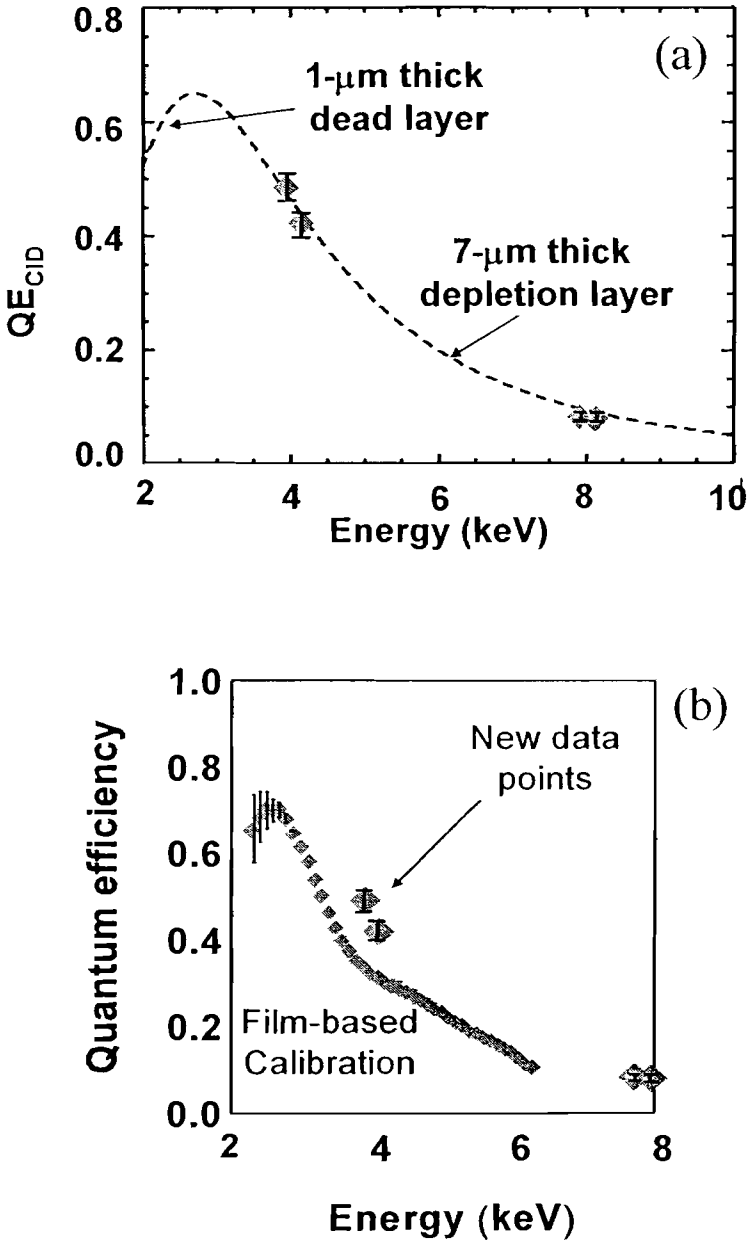
(a)
1-μm thick
dead layer
7-μm thick
depletion layer
QE_{CID}
0.0
0.2
0.4
0.6
0.8
2
4
6
8
10
Energy (keV)
(b)
New data
points
Film-based
Calibration
Quantum efficiency
0.0
0.2
0.4
0.6
0.8
1.0
2
4
6
8
Energy (keV)

Figure 8